Wave influence on altimetry sea level at the coast

Grégoire Abessolo, Florence Birol, Rafaël Almar, Fabien Léger, Erwin Bergsma, Kate Brodie, Rob Holman

Coastal Engineering 180 (2023) 104275

Contents lists available at ScienceDirect

Coastal Engineering

journal homepage: www.elsevier.com/locate/coastaleng

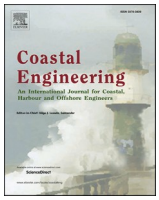

Wave influence on altimetry sea level at the coast

Grégoire O. Abessolo [a,*], Florence Birol [b], Rafael Almar [b], Fabien Léger [b], Erwin Bergsma [c], Kate Brodie [d], Rob Holman [e]

[a] Ecosystems and Fishery Resources Laboratory, Institute of Fisheries and Aquatic Sciences, University of Douala, BP 2701 Douala, Cameroon
[b] LEGOS, OMP, UMR 5566 (CNES-CNRS-IRD-University of Toulouse), Toulouse, France
[c] CNES, 18 Avenue Edouard Bélin, 31400, Toulouse, France
[d] US Army Engineer Research and Development Center, Coastal and Hydraulics Laboratory, 1261 Duck Rd, Duck, NC, 27949, USA
[e] College of Earth, Ocean and Atmospheric Sciences, Oregon State University, 104 Ocean Admin Bldg, Corvallis, OR, 97331-5503, USA

ARTICLE INFO

Keywords:
Coastal altimetry
Sea level
Waves
Video camera
Tide gauge
Buoy
Altimeter
Significant wave height
Re-tracking algorithm

ABSTRACT

Nowadays, in most altimetry sea level products, data are only retrieved up to 5–10 km from the coasts. The need to extend the satellite sea level record closest to land has led to dedicated studies in order to define and develop altimetry processing algorithms adapted to coastal ocean conditions. Among the different issues that strongly affect the performance of satellite altimetry as we approach the coast, the robustness of the correction related to the different states of sea surface waves (called sea state bias) is suspected to be one of the most important. Moreover, waves undergo a series of transformations when propagating from deep-water to shallow water, that add a dynamical contribution to the sea level, known as wave set-up and set-down. This signal impacts altimetry-measured coastal sea level in a way that remains poorly quantified and understood. Here, through a case study, we explore the potential to use the combination of shore-based camera video and tide gauges as a validation and analysis tool for coastal altimetry. The results show that measurements of sea level fluctuations on annual scales is similar between all three datasets. The analysis of the sea level data from both the tide gauge and the video camera which are co-located reveals that the physical contribution due to wave set-up and wave set-down accounts for 2% of the total sea level variations at monthly scale. We observe the loss of quality of the altimetry-derived significant wave height at ~10 km from the coast, confirming the associated loss of accuracy in the sea state bias correction. Finally, this study highlights the critical need to co-locate the various measuring tools and devices at the coast with the satellite ground tracks if we want to optimally exploit coastal altimetry up to the coastline.

1. Introduction

Satellite altimetry has provided measurements of the sea level variations with a global coverage and an accuracy of a few centimeters (Abdalla et al., 2021) for the past 30 years. This observation technique, which provides also wave height and wind speed estimates, was initially developed for the deep ocean, far away from the coast, and has played a crucial role in improving the knowledge of the ocean dynamics at global scale (Fu and Le Traon, 2006). In contrast, in the coastal zone, tide gauges are traditionally used for sea level monitoring (Woodworth et al., 2017). The global network of tide gauges has produced several long-term time series of sea levels, but these observations are unevenly distributed throughout the coastal areas (Vignudelli et al., 2019; Woodworth et al., 2017). Tide gauges are local and do not provide information about the regional sea level context. They are also generally located in sheltered harbors, thus missing a part of sea level variability due to waves (Melet et al., 2018). In addition, it is particularly difficult or expensive to install and/or maintain tide gauges in developing countries or remote places, leading to large data gaps. There is an obvious need to extend the satellite-based sea level record toward the coast, and recent efforts are focused on deriving coastal altimetry data with a quality comparable to that of the open ocean (Vignudelli et al., 2019).

The first difficulty in coastal altimetry data exploitation is the land contamination of altimeter echo waveforms, which is complicated by the inhomogeneity of the reflecting surface (Xu et al., 2019). Another issue is that some of the standard altimetry correction approaches become inaccurate near the coast (Vignudelli et al., 2011). These

* Corresponding author.
E-mail address: gregoireabessolo@ish.cm (G.O. Abessolo).

https://doi.org/10.1016/j.coastaleng.2022.104275
Received 18 February 2022; Received in revised form 21 May 2022; Accepted 27 December 2022
Available online 28 December 2022

corrections include the effects of the wet/dry ionospheric and tropospheric delays (Fernandes et al., 2013), the tidal signal (Ray et al., 2011), the sea state bias (Pires et al., 2018; Chambers, 2015) and the dynamic atmospheric correction (Chambers, 2015; Carrère and Lyard, 2003). To extract a reliable sea level estimate close to the coast, altimetry measurements thus require dedicated and careful processing approaches, and during the last decades, several algorithms have been developed to better exploit near-shore altimetry information (e.g., Peng and Deng 2020, 2018; Marti et al., 2019; Boy et al., 2017; Roscher et al., 2017; Birol et al., 2017; Valladeau et al., 2015; Passaro et al., 2014). These processing algorithms include both dedicated altimeter waveform fitting process, called re-tracking, and altimetry corrections.

However, coastal ocean re-tracking techniques are not yet included in baseline algorithms for the generation of operational sea level products. The sea state bias (*SSB*) correction remains also one of the largest error sources for the global mean sea level (*GMSL*) time series (Cheng et al., 2019) and for regional altimetry (Passaro et al., 2018). *SSB* is a sea level height bias that is due to the presence of waves on the sea surface: reflected radar signals are stronger in the troughs than near the crests of the waves, leading to an underestimation of the sea level. This process varies in a non-linear way as a function of wind speed and wave height, and thus can induce systematic errors due to the local/regional wave/wind characteristics. *SSB* is estimated using an empirical formulation, based on the altimeter significant weight height (*SWH*) and surface wind speed (Vignudelli et al., 2019). These parameters are also derived by the ocean re-tracking technique which performs poorly near the coast, resulting in erroneous *SSB* values. Moreover, the empirical formulation used is derived from open ocean altimetry data analysis and does not take into account coastal sea-state conditions.

Near the coast, waves not only affect the echoes from the radar altimeter's emission on the sea surface, they also affect the sea level itself as waves undergo a series of transformations when propagating from deep-water through intermediate to shallow water. Eventually the wave amplitude, hence steepness, increases until the waves become unstable and break (Dodet et al., 2019) when water-depth becomes too shallow. These transformations are at the origin of the well-known processes of wave set-down and set-up (Raubenheimer et al., 2001; Dean and Walton 2009; Pugh and Woodworth 2014) that are proportional to *SWH*. Wave set-up is the superelevation of the sea level in comparison to mean total sea level owing to the presence of breaking incident waves (Guza and Thornton, 1981) while wave set-down is the depression of the sea level in comparison to mean total sea level seaward of the surf zone (Raubenheimer et al., 2001). These processes are a spatially varying contribution (from one to tens centimetres) to the temporally varying mean total sea level at a given time, with highest magnitudes occurring within 1 km of the coast, where waves are shoaling and breaking.

Presently, most altimetry based sea level products are limited to about 5–10 km from the coast. The rapid improvements in altimetry processing algorithms and in altimetry technology (*e.g.* the new generation of altimeters with a *SAR* measurement mode) allow new experimental coastal altimetry datasets, with sea level estimates even closer to the coast (up to 1–2 km, Birol et al., 2021). However, as these measurements are collected closer to the coast where waves may have a cumulative effect on both the sea level itself and the accuracy of the altimeter measurements, it is increasingly important to understand the impact of shallow and intermediate waves on satellite altimetry sea level measurements. In parallel, new validation tools that could help to understand the main factors that determine the altimetry data accuracy are needed. In particular, optical data from nearshore video cameras have the advantage of being available at a very low cost (Holman and Haller, 2013). Nearshore video cameras show unique potential to monitor at daily scale the spatial variability of sea level in shallow waters (0–10 m-depth) with a spatial coverage ranging from meters to kilometers (Abessolo et al., 2019; Thuan et al., 2019), and could be used for such application.

In this paper, as a first approach, we focus on processes that result in sea level variability at monthly scale. We use the unique availability of shore-based video systems, tide gauge, wave buoys and altimetry at the coastal area of Duck, North Carolina (NC), United States of America (USA), to 1) accurately measure both total sea level at the coast and wave contribution to sea level and 2) explore the potential influence of waves on altimetry-derived sea level measurements at the coast. We investigate whether all contributions to sea level variations at the coast could be captured by analysing co-located data at a single site and how waves might impact altimetry coastal sea level.

2. Data and methods

2.1. Study site

The study site is located at the U.S. Army Engineer Research and Development Center's Field Research Facility (FRF) along the coast of Duck, North Carolina, USA. It is home to several local measuring devices that have recorded time series of data over more than three decades: a shore-based video system composed of several cameras recording since 1986, a tide gauge installed since 1977, and three wave buoys deployed at a depth of 17, 26 and 49 m respectively since 2013, 2008 and 2017 (Fig. 1). There are also five altimetry tracks that pass relatively close to the surveying area around Duck.

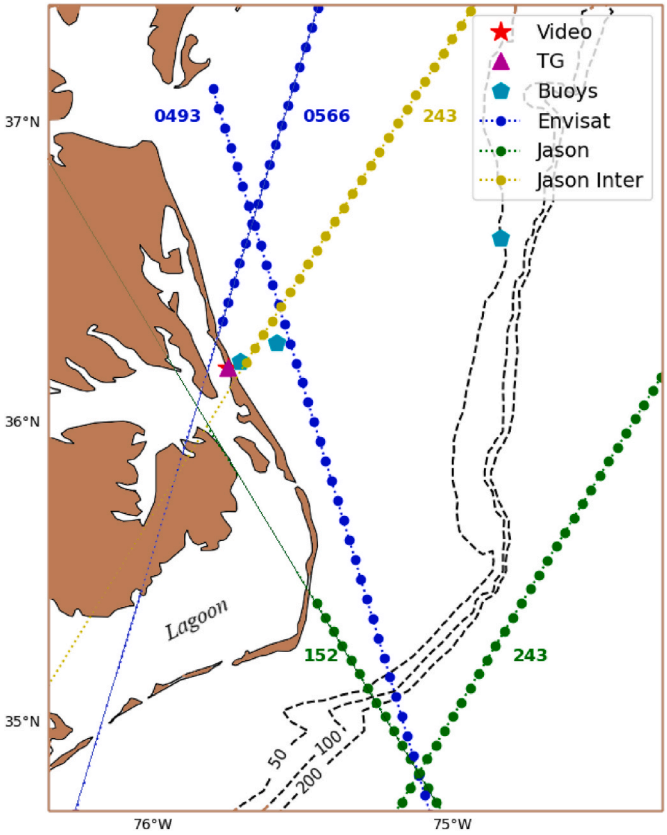

Fig. 1. Study site at Duck, North Carolina, USA. Ground tracks of available closest satellite missions are shown: Jason 1, Jason 2 and Jason 3 tracks 152 and 243 (green), Jason Interleaved track 243 (yellow), Envisat track 566 and Saral/Altika track 493 (blue). Dots stand for the altimetry reference points considered in this study. Red star stands for Argus video system location. Magenta triangle stands for tide gauge location. Sky blue pentagons stand for buoys location (17 m, 26 m and 49 m-depth). Dashed lines stand for depth contours at 50, 100 and 200 m. Distances on the different altimetry tracks are measured from the coast.

2.2. Altimetry data

From all available altimetry tracks in the study area, only the ones crossing the coast were considered here (Table 1). The Envisat and SARAL/Altika tracks 566 and 493 were not used because of the long repeat orbit of these missions, about 35 days, resulting in low data samples. The Jason missions, in contrast, had repeat collects every ~10 days and thus both Jason and Jason interleaved (called Jason 1N) orbits were considered. Data located in the lagoon area along the track 152 for Jason 1, 2 and 3 (a section of ~90 km large) were discarded from the analysis because they are representatives of very local conditions with almost no waves. The tracks and period of time considered for each mission are summarized in Table 1. Note that Jason missions have an inter-track distance of 315 km at the equator. All other missions (e.g. ERS1/2, Topex, GFO) were discarded because they correspond to time periods when the in situ data used in this study were not available. These missions also carried older sensors, known to provide very few observations in coastal areas.

Sea level time-series were extracted along the considered tracks from the CTOH (Center for Topographic Studies of the Ocean and Hydrosphere) along-track coastal altimetry product called X-TRACK (Birol et al., 2017). X-TRACK multi-mission altimetry products were developed with the goal of retrieving altimeter information closer to the coast (Birol et al., 2017). Two versions of the product exist: an experimental high frequency (HF) version at 20 Hz resolution (i.e. a sea level estimate every 350 m in the alongtrack direction) and a mature 1 Hz resolution (a sea level estimate every ~ 6 km in the alongtrack direction) version which is distributed by the AVISO + service. The HF version of the X-TRACK processing chain uses higher rate (and then significantly noisier) altimetry measurements. It has been validated in the framework of the *ESA SL_cci* project (Birol et al., 2021). Compared to the 1-Hz version, the corresponding HF sea level data have a higher noise ratio but allows getting physical information closer to the coast and then to capture more coastal sea level signals (Birol and Delebecque, 2014).

Note that X-TRACK is based on geophysical parameters derived with a classical ocean re-tracking techniques, called *mle4* (Birol et al., 2017). The derived *SWH* time-series are used for comparison to the buoys data in order to analyze their quality when we approach the coast.

The time-series of Jason 1, Jason 2 and Jason 3 have been combined into a single time-series, which we will refer to as Jason 1, 2, 3 in the following. As a reminder, the sea level variations measured at the coast are a superposition of several contributions, namely global to regional sea level anomaly *(SLA)*, local effects of astronomical tides, atmospheric surges (*DAC*), and wave transformations in the surf zone (Abessolo et al., 2019; Melet et al., 2018). In Jason 1, 2, 3 products, the contribution of astronomical tides was removed, by subtracting the tidal amplitudes that were derived from the Global tide FES2012 model (Carrère et al., 2012). A low-pass Lanczos-filter was applied to the derived sea level time-series using a 40-km moving window along the altimetry tracks. To perform the comparison with tide gauge and video sea level measurements, the obtained time-series were first interpolated on video acquisition time, and then monthly averaged.

2.3. Video system and data

The shore-based Argus video system at the FRF has coordinates 36.18269° N and −75.75139° E. The high-resolution video cameras were mounted on the top of the 43 m tall tower. This system has been up-and running in different configurations (updates were done as the technology evolved) ever since the first installation in 1986. The optical intensity time series data that were used for this study, were collected by six video cameras at 2 Hz-frequency. Several ground control points were used for the photogrammetric transformation from pixel coordinates to local ground coordinates. The optical intensity time series data were merged every hour over the period 2010 to 2014 and every 30 min over the period 2015 to 2020 to obtain pixel arrays (Holman and Haller, 2013; Holman and Stanley, 2007), that started to be stored in 2010. The pixel arrays extends 2 km alongshore and 400 m cross-shore over the period from 2010 to 2014 and then 800 m cross-shore from the coast since 2015. The cross-shore distance was measured from the camera location at the coast.

The pixel arrays were processed by applying first a temporal wave celerity-sensing method and second a depth inversion method to estimate the underwater topography. Bergsma and Almar (2018) compared this temporal approach, with the well-known *cBathy* spectral approach (Holman and Haller, 2013) and they observed that both approaches led to similar results in synthetic cases. The time-varying sea levels were estimated as the anomaly that is separated from the daily averaged underwater topography. That is, since wave speed is related to depth and we can assume bathymetry changes slowly during most conditions, variations in depth can be related variations in sea level (see Abessolo et al., 2019 and Thuan et al., 2019 for more details). The obtained video-derived total sea levels were then filtered using a Kalman filter with the implementation of an error proxy that allows the removal of outliers. The proxy is computed as the difference between inverted depths derived from two different principles of celerity estimation (see details in Bergsma and Almar, 2018; Abessolo et al., 2020). The validation of this filtering method showed that the mean square error can be reduced by at least 30% (Abessolo et al., 2020). The filtered video-derived total sea levels were finally smoothed using a 2-h and a 40-m windowed moving-average. The resulting video-derived sea levels are however affected by several physical (*e.g.* limit of validity of the wave dispersion relation, bias of breaking), environmental (e.g. reflection of sunlight on water and fog) and instrumental (intrinsic parameters of the camera such as the distortion) parameters. In Abessolo et al. (2019), the mean square error was about 0.2 m (~10% of the total sea level) over 8 days when compared to in-situ sea level measurements from an Acoustic Doppler Current Profiler (ADCP).

Contribution due to astronomical tides was removed in the same way as in the altimetry data, by subtracting the tidal amplitudes from the video-derived sea levels. The tidal amplitudes were downloaded from the National Oceanic and Atmospheric Administration (NOAA) website. The obtained video time-series were averaged monthly to perform the comparison with altimetry and tide gauge sea level data.

Table 1
Satellite missions considered to derive sea level variations.

Mission	Start date	End data	Tracks
Jason 1	Jan 21, 2002	Jan 22, 2009	152
Jason 2	Jul 17, 2008	Sep 28, 2016	152
Jason 3	Feb 26, 2016	May 21, 2019	152
Jason 1N	Feb 19, 2009	Feb 15, 2012	243

2.4. Tide gauge data

The tide gauge at Duck, North Carolina was installed on December 01st, 1977 and collects data at a 6 min-frequency. It is located on the offshore end of the pier in the National Data Buoy Center trailer at the coordinates 36.18333° N and −75.74667° E. This tide gauge has the advantage of being installed on an open coast and being the closest to the video system location compared to the others long term tide gauges along the North Carolina coast (Oregon inlet Marina on 1974, Beaufort established on 1964, Wilmington established on 1908). The Duck tide-gauge has a solid, well-documented installation and continuous operational history. In addition, the tide gauge is installed in the field of view of the video camera.

In a similar way to altimetry and video measurements, contribution due to astronomical tides was removed by subtracting the tidal amplitudes from the tide gauge measurements. For the comparison with altimetry and video sea level data, the derived time-series were first interpolated on video acquisition time, and then monthly averaged.

2.5. Buoys data

Three directional buoys are located near the Duck tide gauge at the FRF (see Fig. 1): one at 17 m-depth, 3 km from the coast (36.19970 N, −75.71412 E); another at 26 m-depth, 15 km from the coast (36.25881 N, −75.59221 E) and the last at 49 m-depth, 94 km from the coast (36.61100 N, −74.84133 E). All these buoys are located out of the waves set-down and set-up area. However, the collected *SWH* and wave period data can be used to estimate the wave contribution to sea level. The *SWH* dataset used in this study is from the 26 m buoy as it is the buoy with the longest time series (from May 2008) located close to the tide gauge and the altimetry tracks at the coast. The latter collects data every 30 min and shows the following mean wave characteristics: *SWH* 1.18 m, peak period T_p 8.39 s, direction 47°. Buoy data were daily averaged to perform comparison with *SWH* derived from Jason 1, Jason 2, Jason 3 and Jason 1N. The Jason 1, 2 and 3 track is farther away spatially from the FRF and the selected buoy. But, the closest buoy (35.25925 N, −75.2861 E) to this track has only been in place since August 2021, and cannot be used for this study.

2.6. Estimation of contributions to sea level variations

It is commonly accepted that wave-induced coastal sea level changes are insignificant on monthly time scales. But, recent works (Melet et al., 2018, 2020; Ponte et al., 2019; Woodworth et al., 2019) have highlighted that wave set-up, which depends on wave characteristics (height, period and direction), can contributed significantly to coastal sea level changes on longer timescales (interannual-to-multidecadal, including the monthly scale in this study) due to changes in atmospheric circulation patterns and the consequent surface winds, in response to internal climate variability and climate change. Here, we assumed that the wave energy $SWH^2.T_p$ derived from the data collected by the buoy moored at 26 m depth, can be used to estimate the wave-induced sea level changes.

The sea level anomaly (*SLA*) variations were estimated by removing the Dynamic Atmospheric Correction (*DAC*) estimates from tide gauge time-series (tides having been taken out). The *DAC* estimates, that represent the sea surface high frequency response to wind and pressure forcing combined with inverse barometer, were downloaded from the AVISO + website (https://www.aviso.altimetry.fr/en/data/products/auxiliary-products/dynamic-atmospheric-correction.html).

A multiple linear regression (see Angnuureng et al., 2017) was therefore computed as a function of distance to the coast, between the video-derived sea levels (SL_{video}) and the contributors to coastal sea level (*SLA, DAC* and wave energy):

$$SL_{video} = \zeta_0 + \zeta_1.SLA + \zeta_2.DAC + \zeta_3.SWH^2.T_p \quad (1)$$

The ζ_i are the regression coefficients. The *DAC* and the *SLA* contributions were assumed to be constant along the video cross-shore profile.

In order to evaluate the influence of all the contributors to total sea level, the contribution of astronomical tides (derived from the Global tide FES2012 model) have been considered. The relative contribution of each sea level component P_i was estimated from the ratio of the individual variance to the total variance ($\zeta_1.SLA + \zeta_2.DAC + \zeta_3.SWH^2.T_p$).

3. Results

3.1. Sea level variability measured at the coast

Fig. 2 (left) shows the sea level variations derived from altimetry (along track 152 for Jason 1, 2, 3 and along track 243 for Jason 1N) and from the video system between January 2010 and December 2018. Both satellite altimetry sea level records and the video-derived sea level heights are dominated by the sea level annual cycle that may be related to the local temperature or climate, with variability in phase in all data sets. The corresponding standard deviations are reported on Fig. 2 (right), as a function of distance to the coast. The depth evolution is also reported. In the video, the sea level standard deviation vary between 11 and 13.5 cm. In altimetry, Jason 1N shows a greater stability of standard deviations along its track compared to Jason 1, 2, 3. This is probably related to the respective location of the data sets: fully on the continental shelf for Jason 1N, whereas Jason 1, 2, 3 crosses the continental shelf break. Jason 1, 2, 3, also crosses the Gulf Stream current which certainly affects sea level dynamics and drives down similarities. Fig. 2 (right) shows sea level standard deviation increases more than 12.5 m close to shore in Jason 1, 2, 3 and Jason 1N (0–33 km for Jason 1, 2, 3 and 3–8 km for Jason 1N). The sharp increase observed in Jason 1N is probably induced by errors due to land contamination of the altimeter's echo waveforms, however the data quality appear good up to 8 km from the coast. For Jason 1, 2, 3, the change in standard deviation observed is smooth and likely induced by the difference in ocean dynamics between the continental shelf and the area further offshore. The standard deviation of sea level variations derived from all the datasets closest to the

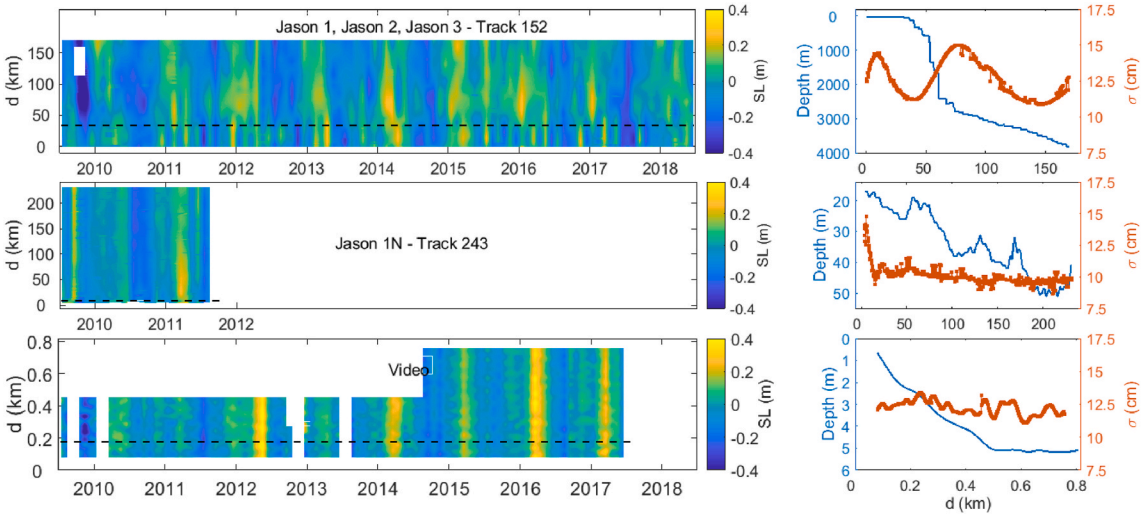

Fig. 2. Shore and near shore sea levels variations (SL) from altimetry (Jason 1, 2, 3 on track 152 and Jason 1N on track 243) and video as a function of distance to the coast and of time at monthly timescale (left panels). Right panels show depth and sea level standard deviation (σ) evolution along the profile in the coastal area for the selected sensor. Black dashed lines show where are the sea level time-series that are the most correlated with the tide gauge data: 33 km from the coast for Jason 1, Jason 2 and Jason 3, 10 km from the coast for Jason 1N, 180 m from the coast for video.

coast, are indicated in Table 2. For video, the sea level standard deviations were averaged along the 800 m-track. From Table 2, the standard deviations of continental shelf sea level variations from tide gauge, Jason 1, 2, 3, and Jason 1N are observed to be quite similar (11, 11.5 and 10.8 cm respectively), if the nearshore sea level increase area is discarded. In this case, the standard deviation from video is larger (12.3 cm), suggesting that the latter captures a sea level contribution that tide gauge and altimetry do not see.

3.2. Validation of altimetry derived sea level variations at the coast with tide gauge and video

Taking a closer look at sea level time series, Fig. 3 shows the comparison between tide gauge data and the most correlated altimetry and video sea level point, that are shown on Fig. 2 (left) with black dashed lines. The comparison reveals that, although the amplitude of sea level variations closest to the coast derived from tide gauge and altimetry are lower than the one derived from video, the sea level annual cycle observed is quite similar in all the data sets. Calculating the correlations and root mean square differences (Table 3) shows that all the data sets appear to capture well the different sources of variability, including *SLA* and *DAC*. However, most of the discrepancies are observed between altimetry and the two other data sets, suggesting that altimetry measurements miss part of the sea level dynamics captured by the other sensors. A first explanation is the temporal resolution of Jason missions (with a revisit time of ~10 days), much lower that the video and the tide gauge. That is, altimetry does not measure the coastal physical mechanisms with the same accuracy as the video and tide gauge. In addition, altimetry tracks are not exactly co-located with tide gauge and video. Jason-1N performs significantly better than Jason 1, 2, 3, probably because it is located very close to the other instruments. But unfortunately, the corresponding time series is much shorter. The Jason 1, 2, 3 track (152) is not only far from the FRF, it is also quite close to the Gulf Stream current which could significantly affect the spatial variability of waves and sea level anomalies. The discrepancies observed between tide gauge and video, even if they are lower, confirm that some physical processes may not be captured in the same way by all the data sets.

In the following analyses, we consider only data at depth shallower than 150 m, and compare monthly time-series of sea level derived from the satellite altimeters along the considered tracks with monthly time-series of sea level from the tide gauge and from the video-derived data (Fig. 4). The considered video time-series was extracted at 180 m from the coast, which was the most correlated ($r = 0.93$) with the tide gauge time-series. Two main observations stand out. First, altimetry derived time-series along the tracks are all similarly correlated with tide gauge and video, except for Jason 1N when approaching the coast (within 50 km), where the correlation with the tide gauge increases significantly. In contrast, within 8 km of the coast, there is a significant decrease in the correlation between Jason 1N and the video that is coincident with the sharp increase in Jason 1N sea level amplitude reported above (Fig. 2, right). The second observation shows that there is an almost constant bias of 0.02 m along the altimetry tracks between the RMS differences computed relative to the video and to the tide gauge. As a result, the altimetry has a higher RMS error with the video than with the tide gauge. All these observations suggest that there is a component (perhaps wave-induced sea level variability) in the video signal that is not present in the tide gauge and altimetry signals, and the influence of this component is stronger near the coast (less than 8 km).

Table 2
Average standard deviation of sea level variations closest to the coast, derived from video, tide gauge and altimetry. Astronomical tide has been removed. Altimetry and tide gauge data were interpolated on video acquisition time.

	Distance range (km)	Depth range (m)	Standard deviation (cm)
Video	[0.1–0.8]	[0.1–5.6]	12.3
Tide gauge	0.4	4.1	11
Jason 1N - 243	[3–8]	[16–18]	12
	[8–28]	[18–22]	10.8
Jason 1, 2, 3–152	[0–33]	[18–62]	13
	[33–53]	[62–770]	11.5

3.3. Wave-induced sea level variability at the coast

An estimate of wave-induced sea level variability (*i.e.* sea level variations without the *SLA*, the *DAC* and the tides) at monthly scale within 1 km of the coast (Fig. 5A) is calculated using a multiple linear regression. The estimated wave-induced sea level variability shows a spatial relationship consistent with the expected pattern of wave setup/set-down. That is, the wave contribution is negative in the region we would expect wave set-down (up to - 0.021 m from 0.4 to 0.7 km from the coast) and makes a positive contribution in the region we would expect wave setup (up to 0.025 m from 0.1 to 0.3 km from the coast). Indeed, the monthly significant wave height conditions vary between 0.5 and 1.9 m and the waves start to shoal/break on average at 3 m-depth, which corresponds to a distance of 0.3 km from the coast. And the observed wave-induced sea level amplitudes are consistent with the literature (Raubenheimer et al., 2001; Dean and Walton 2009). We also estimate the relative contributions of the *DAC* (i.e. sea level variations without the *SLA*, the wave's contribution and the tides) and the *SLA* (i.e. sea level variations without the *DAC*, the wave's contribution and the tides) for comparison. If this time we take into account the tides, the wave contribution represents 2% of the total sea level variations at the coast (Fig. 5B). This spatial variability in the wave-driven contributions to sea level cannot be captured by the tide gauge and altimetry data. The tide gauge measures the sea level at one point whereas the altimetry data are still too far from the coast to be able to observe this wave process. Note that the error bars (Fig. 5A) show the effects of physical, environmental and instrumental parameters that affect the accuracy of video measuring process (Abessolo et al., 2019), in addition to the contribution of coastal and geostrophic currents that are difficult to quantify. These errors were computed as the difference between the observed sea level variations (from the video) and the modelled sea level variations (from the multiple regression).

3.4. Coastal altimetry SWH analysis

Finally, in order to further explore the potential effect of waves on coastal altimetry data, we compare the *SWH* time series derived from the different altimeters using the *mle4* retracker, and from the buoy moored at 26 m depth. Results are reported in Fig. 6. This comparison consists of calculating the correlation and the root mean square differences (RMSE) between the in-situ and altimetry-derived *SWH*. Increasing differences are observed at distances less than ~10 km from the coast for all the altimeters: correlation/*RMSE* values decrease/increase. It indicates a loss of quality in the corresponding altimetry *SWH*. Note that for the typical case of Jason 1, the correlation with buoy measurements seems to be more important because there are only 18 sample measurements considered, as the buoy data are available after May 2008. In terms of coastal *SWH* estimates, the performance of the three altimeters tends to improve from Jason-1 to Jason-3, although these tracks are pretty far from the wave observation locations and waves could be quite different at the same time. In particular, *RMSE* values observed in the 0–10 km coastal band decrease as a function of the mission considered. Anyway, as the altimetry-derived *SWH* is used to compute the *SSB* correction included in operational sea level products, this result confirms that this correction may be a significant source of errors in related coastal sea level data. Obviously, the region concerned is the 0–10 km coastal band.

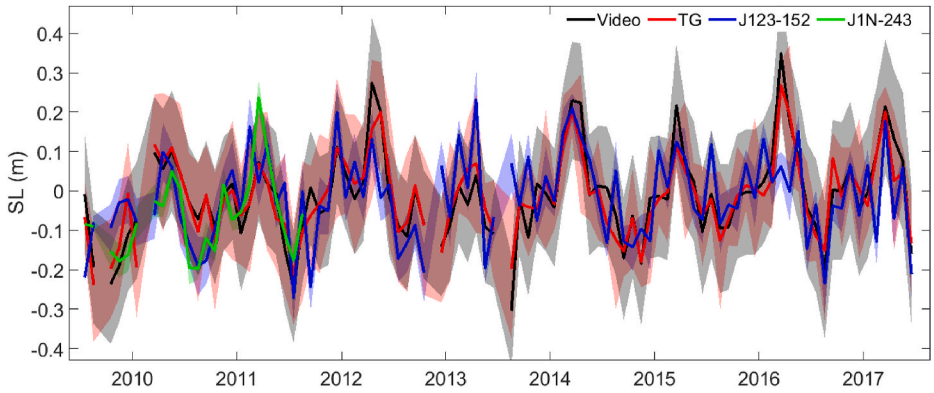

Fig. 3. Comparison between tide gauge data (red) and the most correlated sea level time-series (SL) derived from video (black) and altimetry (blue for Jason 1, 2, 3; green for Jason 1N) at monthly scale. Video and altimetry are extracted at locations shown with black dashed lines on Fig. 2. Shaded areas indicate the day-to-day dispersions within the considered month.

Table 3
Correlations (*r*) and root mean square error (*RMSE*) between tide gauge, video and altimetry derived-sea level variations at monthly scale. Video and altimetry sea level time-series are extracted at locations shown with black dashed lines on Fig. 2 where the correlation is maximum with tide gauge. Astronomical tide has been removed.

r RMSE (m) Period	TG	Video	Jason 1 2, 3 - 152
Video	0.93 0.05 Jan 2010 to Dec 2017		
Jason 1, 2, 3 - 152	0.55 0.10 Jan 2010 to Dec 2017	0.50 0.11 Jan 2010 to Dec 2017	
Jason 1N - 243	0.71 0.08 Jan 2010 to Feb 2012	0.62 0.09 Jan 2010 to Feb 2012	0.78 0.07 Jan 2010 to Feb 2012

4. Discussion

4.1. A new tool to monitor sea level variations at the coast

Altimetry sea level data at the coast are very often validated by comparison with measurements from the nearest tide gauges (*e.g.* Valle-Rodriguez et al., 2020). Compared to altimetry, tide gauges offer a finer temporal resolution and longer records at some locations. However, they are unevenly distributed and do not offer a synoptic view of the sea level variability. The current lack of knowledge on the sea level spatial variability within 10 km of the coast is a critical issue, leading to the need for remote sensing with appropriate resolution in this area. The work presented here shows that having co-located tide gauge and video camera measurements offers the potential to measure the spatial variability of coastal sea level variability and provide new insights on the processes related. Indeed, co-located tide gauge and video measurements opens up possibilities for estimating and understanding the spread of wave contribution to sea level variability within 1 km of the coast. As a result, the physical contribution of wave set-up and set-down to sea level at the coast has been highlighted for the first time through video camera in Fig. 5. This is a major issue because future research efforts are needed to refine estimates of wave set-up and its contribution to total sea level at the coast (Melet et al., 2018) on regional to global scale at longer timescales, instead of using empirical formulas (Melet et al., 2020). It is possible to model these contributions using numerical wave models, but accurate measurements of bathymetry and wave boundary conditions are required to run these models, which may or may not be available depending on location. In order to carry out this study, the *DAC* and *SLA* contributions along the cross-shore profile were assumed to be constant. However, some localized studies have highlighted the variability of these processes closer to the coast. Among others, Cerralbo et al. (2016) have shown through modelling the importance of the cross-shore spatial wind variability in the water circulation in a small-sized micro-tidal bay. In addition, some authors highlighted the influence of river fresh water discharges on sea level at specific coastal locations and that could have effects at larger scale (Piecuch et al., 2020, 2018). These works show the importance of multiplying pilot sites with co-located tide gauges and video systems to

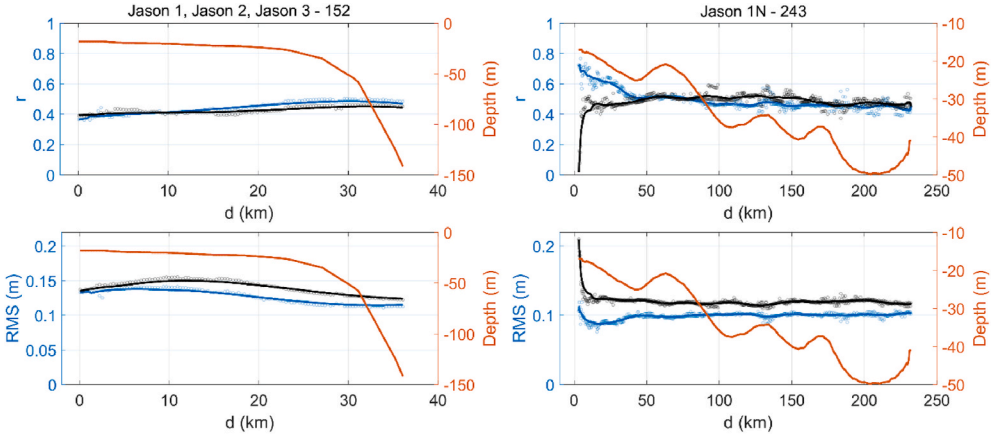

Fig. 4. Validation of altimetry derived sea level variations Top panels compare the correlation coefficient (r, left y-axis) between altimetry and tide gauge time-series (blue) and video-derived time series (black) with depth (red line, right y-axis) and distance from the coast. Bottom panels compare the root-mean-square difference (RMS) for the same quantities. RMS and *r* were smoothed using a 5-km moving window to filter out noise. The video time-series at 180 m represented the most correlated time-series with tide gauge time-series, and was used for comparison purposes here (See Fig. 2). First column of panels stands for Jason 1, Jason 2 and Jason 3 along track 152. The second column of panels stands for Jason-1N along track 243.

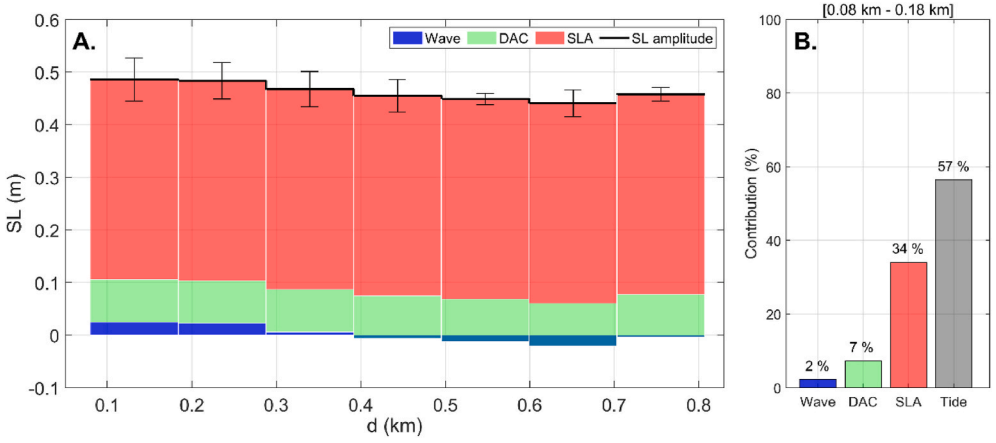

Fig. 5. Contributions to sea level variations derived from the video data at monthly scale. Panel A: time-averaged amplitudes of the contributions to sea level computed along the stack and represented as a function of distance to the coast (in km). The error bars represent the difference between the observed sea level variations from the video and the modelled sea level variations from the multiple regression. Panels B: contribution percentages to total sea level variations from video data at the coast (0.08–0.18 km from the coast). In panel B, the part of astronomical tide has been reported.

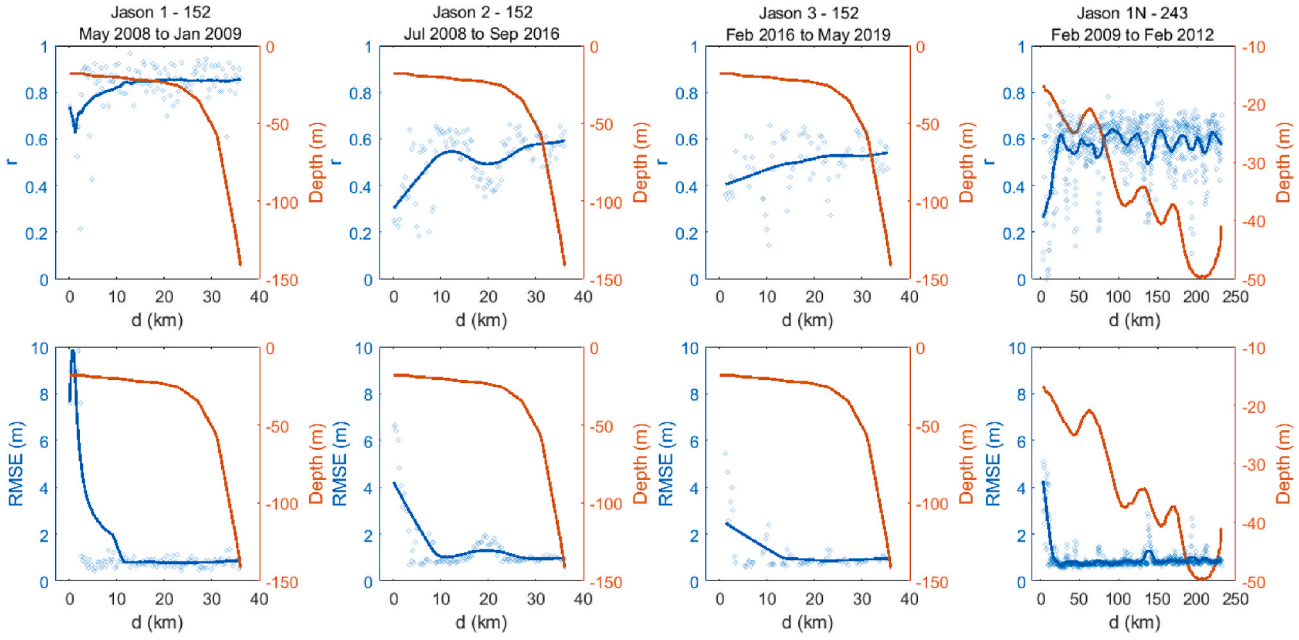

Fig. 6. Comparison between in-situ and altimetry-derived *SWH* for each altimeter (Jason 1, Jason 2, Jason 3 and Jason 1N). The comparison was performed on altimetry acquisition days. Depths were limited to 150 m along the tracks. The first line of panels shows the correlation and the second line the root mean square difference (*RMSE*). In-situ *SWH* time-series were collected using a buoy moored at 26 m.

study the spatial variability of sea level contributors at the coast.

4.2. Towards sea level measurements at the coast co-located with altimetry

The results presented above provide a new method to estimate the performance of coastal altimetry, taking into account all contributions affecting sea level. Today, there are several observations networks along the world's coasts, including tide gauges, buoys, in-situ measurement campaigns, and more recently video systems whose development has accelerated in the last twenty years. And the video camera network is still growing. However, the choice of location for the cameras does not depend on altimetry validation issues. They have no reason to be collocated with the different satellite ground tracks or with the tide gauges. In fact, there are only a few sites where video systems are co-located with tide gauges and altimeter tracks, including Duck site. Therefore, optimizing the location of coastal observing systems in regard to the satellite ground tracks would certainly foster the validation of coastal altimetry measurements. Of course, feasibility could be difficult regarding the additional costs and specific scientific issues related to the localization of observing systems. But co-locate these networks (tide gauges, video and buoys) with altimetry tracks should promote a multi-scale and multi-spatial understanding of processes affecting sea level: beyond 1–5 km from the coast by future altimetry with a time resolution of several days, within 1 km by video camera with a time resolution of a few minutes to a day and at specific fixed locations by tide gauges with high resolution (from minutes to hours). In addition, wave buoys would be used to refine the *SSB* correction at the coast. Such a spatial distribution of observing systems could address many misunderstandings in the literature regarding the coastal zone, and would bridge the gap between the coastal and offshore scientific communities.

4.3. Altimetry waveform re-tracking algorithms

The accuracy of sea levels measurements retrieved at the coast from altimetry missions is obviously determined by the performance of the re-tracking algorithm used. The *mle4* retracker algorithm implemented in the altimetry sea levels products is known to be suboptimal for the

coastal ocean (Tourain et al., 2021; Passaro et al., 2021). We have also seen that, within 10 km from the coast, the altimetry-derived *SWH* estimates become inaccurate, which is expected to impact the *SSB* correction and then finally the sea level. The long-standing debate in the coastal altimetry community regarding the choice of the best re-tracking algorithms is still not resolved as several new algorithms are proposed and tested in the literature (*e.g.* Passaro et al., 2021; Peng and Deng 2020, 2018; Marti et al., 2019). This type of study, extended to different coastal sites, would certainly help to explore their relative performances.

5. Conclusions

This paper investigated how shore-based video systems, tide gauge and altimetry at the coastal area of Duck, NC, USA, respectively measure sea level variations. We also investigate how waves sign on sea level measurements at this coastal site. The results show that all data sets have the same annual signal with discrepancies which could be due to the waves. The wave-induced sea level variations at the coast, that is wave set-up and wave set-down, accounting for 2% of the total sea level variations, was revealed by analysing the sea level data from both the tide gauge and the video camera which are co-located. This study illustrates how co-locate tide gauges and video cameras with altimetry ground tracks might improve a multi-scale understanding of the processes affecting sea level at the coast. The latter is crucial for better assessing present and future coastal sea level rise but requires the availability of altimetry data up to the coastline. Here again, it will be highly beneficial to develop dedicated coastal sites with measurements from shore-based video or Lidar stations, wave buoys and tide gauges collocated with altimetry ground tracks. It will allow to analyze the relative performances of the different algorithms developed for processing coastal altimetry data, define the best ones and finally fully explore the capability of satellite altimetry to complement the other observing systems in coastal sea level studies.

CRediT author statement

G. O. Abessolo: Conceptualization, Investigation, Methodology, Software, Validation, Formal analysis, Resources, Data Curation, Writing - Original Draft, Writing - Review & Editing, Visualization.**: F. Birol**: Conceptualization, Methodology, Validation, Investigation, Resources, Data Curation, Writing - Review & Editing, Funding acquisition, Supervision.**: R. ALmar**: Conceptualization, Methodology, Validation, Investigation, Resources, Data Curation, Writing - Review & Editing, Supervision.**: F. Léger**: Conceptualization, Software, Validation, Resources, Writing - Review & Editing, Visualization.**: E. Bergsma**: Conceptualization, Methodology, Validation, Resources, Writing - Review & Editing.**: K. Brodie**: Resources, Validation, Writing - Review & Editing.**: R. Holman**: Resources, Validation, Writing - Review & Editing.

Declaration of competing interest

The authors declare that they have no known competing financial interests or personal relationships that could have appeared to influence the work reported in this paper.

Acknowledgements

The authors are grateful to the Center for Topographic studies of the Ocean and Hydrosphere (CTOH) at LEGOS (Toulouse, France) for providing the altimetry 20-Hz X-TRACK dataset. Thanks are due to the Coastal Data Information Program (CDIP) for providing free access free access to the buoy data (https://cdip.ucsd.edu/m/products/). We are grateful to the National Oceanic and Atmospheric Administration (NOAA) for providing free access to tide data (https://tidesandcurrents.noaa.gov/). We are also grateful to AVISO + for providing dynamic atmospheric correction data (https://www.aviso.altimetry.fr/en/data/products/auxiliary-products/dynamic-atmospheric-correction.html).

References

Abdalla, S., Kolahchi, A.A., Ablain, M., Adusumilli, S., Bhowmick, S.A., Alou-Font, E., Amarouche, L., et al., 2021. Altimetry for the future: building on 25 years of progress. Adv. Space Res. 68 (2), 319–363. https://doi.org/10.1016/j.asr.2021.01.022.

Abessolo, G.O., Almar, R., Castelle, B., Testut, L., Léger, F., Sohou, Z., Bonou, F., Bergsma, E.W.J., Meyssignac, B., Larson, M., 2019. sea level at the coast from video-sensed waves: comparison to tidal gauges and satellite altimetry. J. Atmos. Ocean. Technol. 36, 1591–1603. https://doi.org/10.1175/JTECH-D-18-0203.1.

Abessolo, O.G., Almar, A., Bonou, B., Bergsma, E., 2020. Error proxies in video-based depth inversion: temporal celerity estimation. In: Malvárez, G., Navas, F. (Eds.), J. Coast Res. Special Issue 95, 1101–1105. https://doi.org/10.2112/SI95-214.1. Coconut Creek (Florida), ISSN 0749-0208.

Angnuureng, D., Almar, R., Sénéchal, N., Castelle, B., Appeaning Addo, K., Marieu, V., 2017. Shoreline evolution under sequences of storms from video observations at a meso-macrotidal barred beach. Geomorphology 290, 265–276. https://doi.org/10.1016/j.geomorph.2017.04.007.

Bergsma, E.W.J., Almar, R., 2018. Video-based depth inversion techniques, a method comparison with synthetic cases. Coast Eng. 138. https://10.1016/j.coastaleng.2018.04.025.

Birol, F., Delebecque, C., 2014. Using high sampling rate (10/20 Hz) altimeter data for the observation of coastal surface currents: a case study over the northwestern Mediterranean Sea. J. Mar. Syst. 129, 318–333. https://doi.org/10.1016/j.jmarsys.2013.07.009.

Birol, F., Fuller, N., Lyard, F., Cancet, M., Nino, F., Delebecque, C., Fleury, S., Toublanc, F., Melet, A., Saraceno, M., Léger, F., 2017. Coastal applications from nadir altimetry: example of the X-TRACK regional products. Adv. Space Res. 59 (4), 936–953. https://doi.org/10.1016/j.asr.2016.11.005.

Birol, F., Léger, F., Passaro, M., Cazenave, A., Niño, F., Calafat, F.M., Shaw, A., Legeais, J.-F., Gouzenes, Y., Schwatke, C., Benveniste, J., 2021. The X-TRACK/ALES multi-mission processing system: new advances in altimetry towards the coast. Adv. Space Res. 455 https://doi.org/10.1016/j.asr.2021.01.049.

Boy, F., Desjonquéres, J.-D., Picot, N., Moreau, T., Raynal, M., 2017. CryoSat-2 SAR-mode over oceans: processing methods, global assessment, and benefts. IEEE Trans. Geosci. Rem. Sens. 55 (1), 148–158. https://doi.org/10.1109/TGRS.2016.2601958.

Carrère, L., Lyard, F., 2003. Modeling the barotropic response of the global ocean to atmospheric wind and pressure forcing-comparisons with observations. Geophys. Res. Lett. https://doi.org/10.1029/2002gl016473.

Carrère, L., Lyard, F., Cancet, M., Guillot, A., Roblou, L., 2012. FES2012: a new global tidal model taking taking advantage of nearly 20 years of altimetry. In: Proceedings of Meeting "20 Years of Altimetry (Venice).

Cerralbo, P., Espino, M., Grifoll, M., 2016. Modeling circulation patterns induced by spatial cross-shore wind variability in a small-size coastal embayement. Ocean Model. 104, 84–98. https://doi.org/10.1016/j.ocemod.2016.05.011.

Chambers, D.P., 2015. Gravimetric methods – satellite altimeter measurements. Elsevier, 117-149. https://doi.org/10.1016/B978-0-444-53802-4.00063-4.

Cheng, Y., Xu, Q., Gao, L., Li, X., Zou, B., Liu, T., 2019. sea state bias variability in satellite altimetry data. Rem. Sens. 11, 1176. https://doi.org/10.3390/rs11101176.

Dean, R.G., Walton, T.L., 2009. Wave setup. In: Handbook of Coastal and Ocean Engineering. World Scientific Publishing Co. Ltd, pp. 1–23. https://doi.org/10.1142/9789812819307_0001 (Chapter 1).

Dodet, G., Melet, A., Ardhuin, F., Bertin, X., Idier, D., Almar, R., 2019. The contribution of wind generated waves to coastal sea level changes. Surv. Geophys. 40, 1563–1601. https://doi.org/10.1007/s10712-019-09557-5.

Fernandes, M.J., Pires, N., Lázaro, C., Nunes, A.L., 2013. Tropospheric delays from GNSS for application in coastal altimetry. Adv. Space Res. 51 (8), 1352–1368. https://doi.org/10.1016/j.asr.2012.04.025.

Fu, L.L., Le Traon, P.Y., 2006. Satellite altimetry and ocean dynamics. Compt. Rendus Geosci. 338 (Issues 14–15), 1063–1076. https://doi.org/10.1016/j.crte.2006.05.015. ISSN 1631-0713.

Guza, R.T., Thornton, E.B., 1981. Wave set-up on a natural beach. J. Geophys. Res. 86 (C5), 4133–4137. https://doi.org/10.1029/JC086iC05p04133.

Holman, R.A., Haller, M., 2013. Remote sensing of the nearshore. Ann. Rev. Mar. Sci 5, 95–113. https://doi.org/10.1146/annurevmarine-121211-172408.

Holman, R., Stanley, J., 2007. The history and technical capabilities of Argus. Coast Eng. 54, 477–491.

Marti, F., Cazenave, A., Birol, F., Passaro, M., Leger, F., Beneviste, F.J., Legeais, J.F., 2019. Altimetry-based sea level trends along the coasts of Western Africa. Adv. Space Res. https://doi.org/10.1016/j.asr.2019.05.033.

Melet, A., Meyssignac, B., Almar, R., Le Cozannet, G., 2018. Under-estimated wave contribution to coastal sea-level rise. Nat. Clim. Change 8, 234–239. https://doi.org/10.1038/s41558-018-0088-y.

Melet, A., Almar, R., Hemer, M., Le Cozannet, G., Meyssignac, B., Ruggiero, P., 2020. Contribution of wave setup to projected coastal sea level changes. J. Geophys. Res.: Oceans 125, e2020JC016078. https://doi.org/10.1029/2020JC016078.

Passaro, M., Cipollini, P., Vignudelli, S., Quartly, G.D., Snaith, H.M., 2014. ALES: a multi-mission adaptive subwaveform retracker for coastal and open ocean altimetry, 2014 Remote Sens. Environ. 145, 173–189. https://doi.org/10.1016/j.rse.2014.02.008.

Passaro, M., Nadzir, Z.A., Quartly, G.D., 2018. Improving the precision of sea level data from satellite altimetry with high-frequency and regional sea state bias corrections. Remote Sens. Environ. 218, 245–254. https://doi.org/10.1016/j.rse.2018.09.007.

Passaro, M., Hemer, M.A., Quartly, G.D., Schwatke, C., Dettmering, D., Seitz, F., 2021. Global coastal attenuation of wind-waves observed with radar altimetry. Nat. Commun. 12, 3812. https://doi.org/10.1038/s41467-021-23982-4.

Peng, F., Deng, X., 2018. Validation of improved significant wave heights from the Brown-Peaky (BP) retracker along the east coast of Australia. Rem. Sens. 10 (7), 1072. https://doi.org/10.3390/rs10071072.

Peng, F., Deng, X., 2020. Improving precision of high-rate altimeter sea level anomalies by removing the sea state bias and intra-1-Hz covariant error. Remote Sens. Environ. 251, 112081 https://doi.org/10.1016/j.rse.2020.112081.

Piecuch, C.G., Wadehra, R., 2020. Dynamic sea level variability due to seasonal River discharge: a preliminary global ocean model study. Geophys. Res. Lett. 47 (4), e2020GL086984 https://doi.org/10.1029/2020GL086984.

Piecuch, C.G., Bittermann, K., Kemp, A.C., Ponte, R.M., Little, C.M., 2018. River discharges effects on United States Atlantic and Gulf coast sea-level changes. Proc. Natl. Acad. Sci. USA 115 (30), 7729–7734. https://doi.org/10.1073/pnas.1808428118.

Pires, N., Fernandes, M.J., Gommenginger, C., Scharroo, R., 2018. Improved sea state bias estimation for altimeter reference missions with altimeter-only three-parameter models. IEEE Trans. Geosci. Rem. Sens. 99, 1–15. https://doi.org/10.1109/TGRS.2018.2866773.

Ponte, R.M., Carson, M., Cirano, M., Domingues, C.M., Jevrejeva, S., Marcos, M., Mitchum, G., van de Wal, R.S.W., Woodworth, P.L., Ablain, M., Ardhuin, F., Ballu, V., Becker, M., Benveniste, J., Birol, F., Bradshaw, E., Cazenave, A., de Mey-Frémaux, P., Durand, F., Ezer, T., Fu, L.L., Fukumori, I., Gordon, K., Gravelle, M., Griffies, S.M., Han, W., Hibbert, A., Hughes, C.W., Idier, D., Kourafalou, V.H., Little, C.M., Matthews, A., Melet, A., Merrifield, M., Meyssignac, B., Minobe, S., Penduff, T., Picot, N., Piecuch, C., Ray, R.D., Rickards, L., Santamaría-Gómez, A., Stammer, D., Staneva, J., Testut, L., Thompson, K., Thompson, P., Vignudelli, S., Williams, J., Williams, S.D.P., Wöppelmann, G., Zanna, L., Zhang, X., 2019. Towards comprehensive observing and modeling systems for monitoring and predicting regional to coastal sea level. Front. Mar. Sci. 6, 437. https://doi.org/10.3389/fmars.2019.00437.

Pugh, D.T., Woodworth, P.L., 2014. Sea-level Science: Understanding Tides, Surges, Tsunamis and Mean Sea-Level Changes. Cambridge University Press, Cambridge, ISBN 9781107028197.

Raubenheimer, B., Guza, R.T., Elgar, S., 2001. Field observations of wave-driven setdown and setup. J. Geophys. Res. 106 (C3), 4629–4638. https://doi.org/10.1029/2000JC000572.

Ray, R.D., Egbert, G.D., Erofeeva, S.Y., 2011. Tide predictions in shelf and coastal waters: status and prospects. Coast altimetry. https://doi.org/10.1007/978-3-642-12796-0_8.

Roscher, R., Uebbing, B., Kusche, J., 2017. STAR: spatio-temporal altimeter waveform retracking using sparse representation and conditional random fields. Remote Sens. Environ. 201, 148–164. https://doi.org/10.1016/j.rse.2017.07.024.

Thuan, D.H., Almar, R., Marchesiello, P., Viet, N.T., 2019. Video sensing of nearshore bathymetry evolution with error estimate. J. Mar. Sci. Eng. 7, 233. https://doi.org/10.3390/jmse7070233.

Tourain, C., Piras, F., Ollivier, A., Hauser, D., Poisson, J.C., Boy, F., Thibaut, P., Hermozo, L., Tison, C., 2021. Benefits of the Adaptive algorithm for retracking altimeter nadir echoes: results from simulations and CFOSAT/SWIM observations. In: IEEE Transactions on Geoscience and Remote Sensing. Institute of Electrical and Electronics Engineers. https://doi.org/10.1109/TGRS.2021.3064236.

Valladeau, G., Thibaut, P., Picard, B., Poisson, J.C., Tran, N., Picot, N., Guillot, A., 2015. Using SARAL/AltiKa to improve Ka-band altimeter measurements for coastal zones, hydrology and ice: the PEACHI prototype. Mar. Geodes. 38, 124–142. https://doi.org/10.1080/01490419.2015.1020176.

Valle-Rodriguez, J., Trasvina-Castro, A., 2020. Sea level anomaly measurements from satellite coastal altimetry and tide gauges at the entrance of the gulf of California. Adv. Space Res. 1593–1608. https://doi.org/10.1016/j.asr.2020.06.031.

Vignudelli, S., Kostianoy, A.G., Cipollini, P., Benveniste, J., 2011. Coastal Altimetry. Springer, Berlin. https://doi.org/10.1007/978-3-642-12796-0.

Vignudelli, S., Birol, F., Benveniste, J., Fu, L.-L., Picot, N., Raynal, M., Roinard, H., 2019. Satellite altimetry measurements of sea level in the coastal zone. Surv. Geophys. https://doi.org/10.1007/s10712-019-09569-1.

Woodworth, P.L., Hunter, J.R., Marcos, M., Caldwell, P., Menéndez, M., Haigh, I., 2017. Towards a global higher-frequency sea level dataset. Geosci. Data J. 3, 50–59. https://doi.org/10.1002/gdj3.42.

Woodworth, P., Melet, A., Marcos, M., Ray, R.D., Wöppelmann, G., Sasaki, Y.N., Cirano, M., Hibbert, A., Huthnance, J.M., Montserrat, S., Merrifield, M.A., 2019. Forcing factors affecting sea level changes at the coast. Surv. Geophys. 40 (6), 1351–1397. https://doi.org/10.1007/s10712-019-09531-1.

Xu, X.-Y., Xu, K., Xu, Y., Shi, L.-W., 2019. Coastal altimetry: a promising technology for the coastal oceanography community. In: Estuaries and Coastal Zones – Dynamics and Response to Environmental Changes. https://doi.org/10.5772/intechopen.89373.